Molecular beam epitaxy and structural anisotropy of m -plane InN grown on free-standing GaN

G. Koblmüller, A. Hirai, F. Wu, C. S. Gallinat, G. D. Metcalfe, H. Shen, M. Wraback, and J. S. Speck

Citation: Applied Physics Letters **93**, 171902 (2008); doi: 10.1063/1.3001806
View online: http://dx.doi.org/10.1063/1.3001806
View Table of Contents: http://scitation.aip.org/content/aip/journal/apl/93/17?ver=pdfcov
Published by the AIP Publishing

Molecular beam epitaxy and structural anisotropy of *m*-plane InN grown on free-standing GaN

G. Koblmüller,[1,a)] A. Hirai,[1] F. Wu,[1] C. S. Gallinat,[1] G. D. Metcalfe,[2] H. Shen,[2] M. Wraback,[2] and J. S. Speck[1]
[1]*Materials Department, University of California, Santa Barbara, California 93106-5050, USA*
[2]*U. S. Army Research Laboratory, Sensors and Electron Devices Directorate, 2800 Powder Mill Road, Adelphi, Maryland 20783, USA*

(Received 9 September 2008; accepted 25 September 2008; published online 27 October 2008)

This study reports on the growth of high-quality nonpolar *m*-plane $[1\bar{1}00]$ InN films on free-standing *m*-plane GaN substrates by plasma-assisted molecular beam epitaxy. Optimized growth conditions (In/N ratio ~ 1 and $T = 390-430$ °C) yielded very smooth InN films with undulated features elongated along the $[11\bar{2}0]$ orientation. This directionality is associated with the underlying defect structure shown by the anisotropy of x-ray rocking curve widths parallel to the $[11\bar{2}0]$ (i.e., 0.24°–0.34°) and [0001] (i.e., 1.2°–2.7°) orientations. Williamson–Hall analysis and transmission electron microscopy identified the mosaic tilt and lateral coherence length and their associations with different densities of dislocations and basal-plane stacking faults. Ultimately, very low band gap energies of ~ 0.67 eV were measured by optical absorption similar to the best *c*-plane InN. © *2008 American Institute of Physics*. [DOI: 10.1063/1.3001806]

With the revision of the band gap energy of InN to approximately 0.7 eV[1] and its small electron effective mass to $\sim 0.05m_0$,[2] this material has become an attractive candidate for optoelectronic, and high electron mobility applications. Most works performed to fabricate good InN films concentrated on the polar wurtzite *c*-plane orientations, i.e., In-face and N-face InN, since appropriate substrates such as *c*-plane sapphire, SiC, or free-standing *c*-plane GaN were readily available. Despite substantial advancements of many physical properties, i.e., electron mobilities higher than 3500 $cm^2/V\,s$[3] and band gap energies lower than 0.65 eV,[4] two severe problems for *c*-oriented (i.e., [0001]) InN have set limits to their commercial applicability.

First, the presence of internal electric fields caused by discontinuities in the polarization along the *c* axis resulted in many drawbacks for In-containing nitride devices. Specifically, the large band bending and reduced overlap in electron-hole wave functions in [0001]-oriented quantum wells yielded undesired shifts in the emission spectra and increased nonradiative recombination.[5] Second, the Fermi level pinning at surface states at ~ 0.7 eV above the conduction band minimum (CBM)[6] demonstrated that *c*-plane InN surfaces contain large electron accumulation.[7,8] This strong *n*-type surface conductivity has heavily obscured both fabrication and analysis of pure *p*-type InN.[9]

To avoid these situations, recent work highlighted that growth of (In)GaN-based heterostructures along nonpolar, i.e., the *a*-plane $[11\bar{2}0]$[10] and *m*-plane $[1\bar{1}00]$[11,12], orientations enhanced nitride devices substantially by eliminating the polarization-induced electric fields. Theoretical calculations[13] predicted also an absence of Fermi level pinning above the CBM for nonpolar orientations, especially for *m*-plane InN. Despite these apparent promises of nonpolar InN, their growth was only rarely reported, i.e., there are few, if any, reports on *m*-plane InN films, while some reports dealt with highly defective *a*-plane InN films grown on *r*-plane sapphire by molecular beam epitaxy (MBE).[14,15]

In this letter, we report on the growth of high-quality *m*-plane InN films on *m*-plane GaN substrates by plasma-assisted (PA) MBE. By identifying optimum growth conditions, good structural quality and band gap energies as low as 0.65 eV could be achieved. Special emphasis was also placed on the inherent film mosaic anisotropy and its correlation with planar and extended defects.

All *m*-plane InN films were grown in a Varian Gen-II MBE system using standard elemental effusion cells for In and Ga while active nitrogen was supplied by a Veeco Unibulb radio-frequency plasma source with a N limited growth rate of 7.2 nm/min. The *m*-plane GaN substrates used in this study were prepared at Mitsubishi Chemical Co., Ltd. by slicing a low-defect bulk GaN crystal along its *c*-direction. The on-axis substrates were specified with threading dislocation (TD) and *n*-type carrier densities of $\sim 5\times 10^6$ cm^{-2} and mid-10^{17} cm^{-3}, respectively. Prior to the InN growth, a 20-nm-thin Ga-rich GaN nucleation layer was grown at 680 °C for good interface quality.

We explored a set of growth temperatures between 390–450 °C at constant In/N flux ratio of ~ 1. By monitoring the growth using reflection-high energy electron diffraction (RHEED) along the $[11\bar{2}0]$ azimuth, the intensity and streak spacing, i.e., strain relaxation profiles, indicated a Stranski–Krastanow growth mode transition at ~ 2 monolayers (ML) of InN, as also observed for *c*-plane InN growth.[16] The formed three-dimensional islands coalesced quickly into a continuous film at around 5–10 nm of growth shown by a transition to its original streaky RHEED pattern. While for growth temperatures below ~ 430 °C, no further change in RHEED intensity was observed throughout the consecutive growth, temperatures higher than ~ 430 °C yielded a gradual decrease in the RHEED intensity contrast. This was associated with the accumulation of In droplets[17] as confirmed for a thick *m*-plane InN film grown at ~ 445 °C. The propensity for In droplets under conditions without excess In flux (i.e.,

[a)]Author to whom correspondence should be addressed. Electronic mail: gregor@engineering.ucsb.edu.

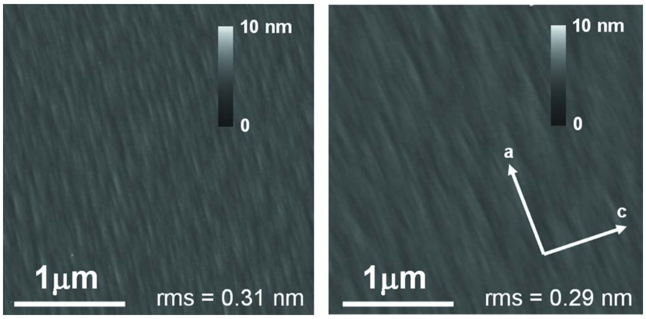

FIG. 1. (Color online) AFMs of the surfaces of ~0.5-μm-thick *m*-plane InN layers grown on *m*-GaN at (a) $T=395$ °C and (b) $T=415$ °C. Note the very low rms surface roughness and morphological anisotropies along *a*- and *c*-directions.

In/N ≤ 1) results usually from thermal decomposition of the InN crystal.[17] The temperature 430 °C thus represents an onset for thermal decomposition, which is much lower than that reported for *c*-plane InN, i.e., ~500 °C for In-face InN[18] and >560 °C for N-face InN.[17,19]

For the *m*-plane InN films grown below the thermal decomposition limit, their surfaces showed atomically smooth morphologies, as obvious from the atomic force micrographs (AFM) in Fig. 1. These images were taken from ~0.5-μm-thick InN films grown at (a) $T=395$ °C and (b) $T=415$ °C after they were etched by a short 20-s-long HCl dip to selectively remove any excess metal In adlayer. Surprisingly, low surface root-mean-square (rms) roughness of ~0.3 nm were measured from the 3×3 μm^2 AFM scans, which are much lower than commonly reported for PAMBE-grown *c*-plane InN surfaces.[18,19] Undulated features elongated along the *a*-direction were observed with step heights of ~0.6–1.3 nm (corresponding to ~2–4 ML of *m*-InN, where 1 ML equals $\sqrt{3}a/2 \approx 3.07$ Å) and widths of ~50–90 nm. The directionality of these undulated features evidences strong morphological anisotropy parallel to the *a*- and *c*-directions similar to the typical slatelike morphology observed for *m*-plane GaN on γ-$LiAlO_2$[20] or *m*-plane SiC.[21] Moreover, the surface undulations were attributed to significant densities of basal-plane stacking faults (BPSFs) (as further discussed below).[22]

The band gap energy of these *m*-plane InN films exhibited very low values similar to *c*-plane InN. Both room temperature optical absorption and photoluminescence (PL) spectra of a ~2-μm-thick *m*-plane InN film grown at $T=415$ °C (Fig. 2) indicated a band gap energy of 0.67 eV and PL peak energy of 0.605 eV. The redshift of the PL peak with regard to the band gap implies that the emission may be related largely to bandtail states. All films grown within the investigated thickness range of 0.5–2 μm resulted in consistently low band gap energies between 0.65–0.69 eV and PL peak energies between 0.605–0.617 eV.

Investigating the structural quality by x-ray diffraction, Fig. 3(a) shows $(1\bar{1}00)$ XRD ω-2θ scans of the three nominally ~0.5-μm-thick *m*-plane InN films described above. Well-resolved diffraction peaks were observed from both the *m*-plane InN $(10\bar{1}0)$ films and GaN $(10\bar{1}0)$ substrates without any (0001) oriented domains. For the InN film grown in the thermal decomposition regime ($T=445$ °C), an additional peak was observed at $\omega \sim 16.5°$. This peak was commonly associated with a tetragonal (101) phase of In metal[23] due to the In droplets on the surface.

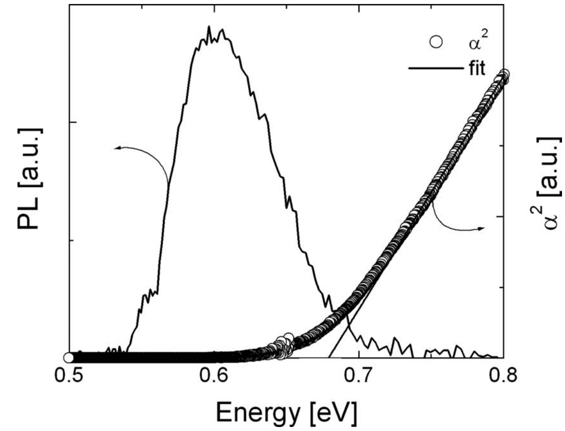

FIG. 2. Optical absorption and PL spectra at 300 K for an ~2-μm-thick *m*-plane InN film with a band gap of ~0.67 eV and PL peak energy of ~0.60 eV.

XRD $(1\bar{1}00)$, $(2\bar{2}00)$, and $(3\bar{3}00)$ rocking curves (ω scans) were also taken along the two orthogonal in-plane [0001] and $[11\bar{2}0]$ orientations. Representative $(1\bar{1}00)$ scans are shown in Fig. 3(b) for the *m*-plane InN film grown at $T=415$ °C, demonstrating a large anisotropy in the rocking curve broadening. In general, the rocking curve broadening

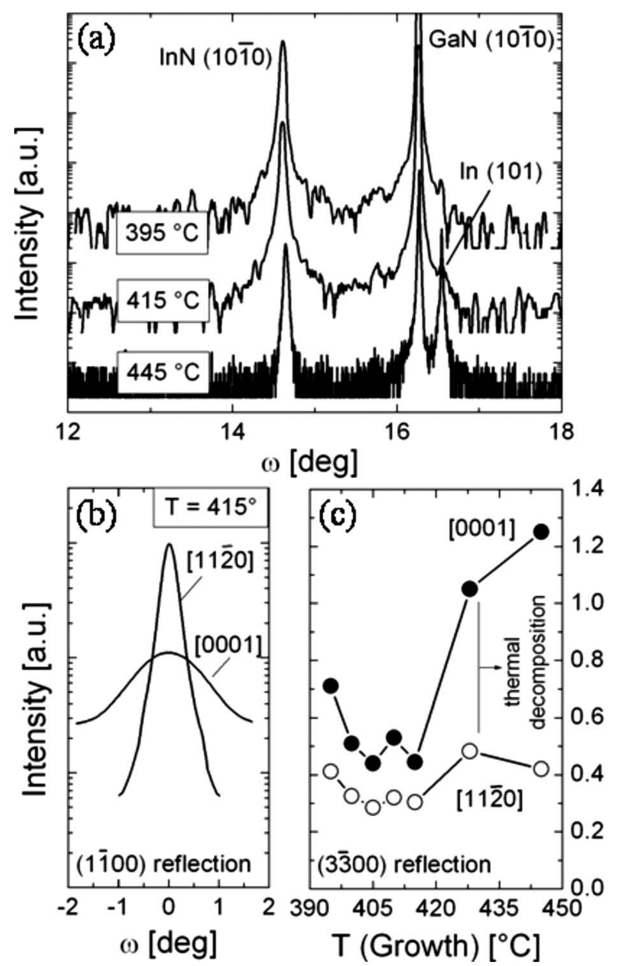

FIG. 3. (a) ω-2θ XRD scans of ~0.5-μm-thick *m*-plane InN films grown on *m*-plane GaN as a function of growth temperature. (b) $(1\bar{1}00)$ rocking curves (ω scans) of the *m*-plane InN peak taken with an open detector parallel to the *a*-direction $[11\bar{2}0]$ and *c*-direction [0001] showing significant anisotropy. (c) FWHM values of the SF-insensitive $(3\bar{3}00)$ rocking curves along these two orthogonal directions as a function of growth temperature.

TABLE I. Summarized results from XRD rocking curves and WH analysis for the a-[11$\bar{2}$0] and c-[0001] directions. Values are given for the rocking curve widths, the LCL, and corresponding SF density.

T(Growth) (°C)	$\Delta\omega(1\bar{1}00)$ a,c (deg)	$\Delta\omega(3\bar{3}00)$ a,c (deg)	LCL (nm)	ρ(SF) (cm^{-1})
395	0.31, 1.86	0.41, 0.71	51	1.95×10^5
405	0.24, 1.26	0.28, 0.44	48	2.1×10^5
410	0.28, 1.58	0.32, 0.53	21	4.7×10^5
415	0.29, 1.62	0.30, 0.45	29	3.4×10^5
445	0.34, 2.77	0.42, 1.25	6	1.6×10^6

$\Delta\omega$ contains contributions from crystal mosaic tilt ($\Delta\omega^{\mathrm{tilt}}$) and stacking-fault-related lateral coherence length (LCL) (L). The mosaic tilt $\Delta\omega^{\mathrm{tilt}}$ was derived from the full width at half maximum (FWHM) of the (3$\bar{3}$00) reflection, which is entirely insensitive to stacking-fault-related anisotropic broadening.[24] The FWHM values of (3$\bar{3}$00) rocking curves measured along the a-([11$\bar{2}$0]) and c-([0001]) orientations are plotted in Fig. 3(c) for a set of samples grown at different temperatures. Similar trends for the FWHMs were identified for both orientations, i.e., near-constant FWHMs with small anisotropy between the a- and c-orientations for low growth temperatures, while much larger anisotropy was observed for temperatures above ~430 °C. The larger anisotropy is most likely related to the large thermal decomposition deteriorating the overall crystal quality similar to c-plane InN.[25]

The contribution of stacking faults to the rocking curve broadening was evaluated via Williamson–Hall (WH) analysis of selected (1$\bar{1}$00) and (2$\bar{2}$00) rocking curve widths. From the linear dependencies of the FWHMs as a function of different reflection orders and their intercept with the ordinate for each data set, we calculated the LCL especially for the [0001] orientation. The LCL and corresponding SF density (1/LCL) varied between 6 and 50 nm and $\sim2\times10^5-1.6\times10^6$ cm^{-1}, respectively (Table I). No direct correlation was identified between $\Delta\omega^{\mathrm{tilt}}$ and LCL since films grown at low temperature, i.e., 395 °C$<T<$415 °C, showed relatively large LCL despite significantly deviating mosaic tilt. But according to the very large mosaic tilt for films grown at $T>$430 °C [compare Fig. 3(c)], the LCL became very small and the SF density became very high.

Figure 4 shows the cross-sectional transmission electron microscopy (TEM) micrographs under different diffraction conditions for a film grown at T=395 °C, indicating a significant TD network with many closed loops within the first ~100 nm of InN growth [Fig. 4(a)] and many basal-plane SFs propagating as straight lines to the surface [Fig. 4(b)].

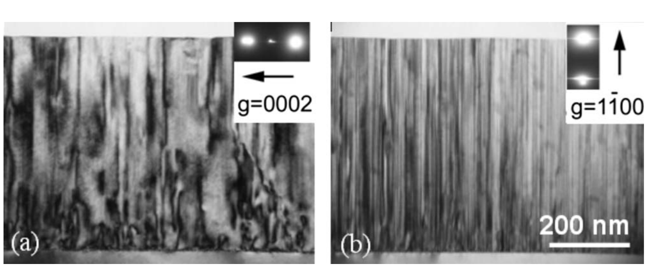

FIG. 4. Cross-sectional TEM images for the [11$\bar{2}$0] zone axis at g=0002 and g=1$\bar{1}$00 diffraction conditions from an m-plane InN film grown at T=395 °C on m-plane GaN.

The density of SFs was determined to be $\sim2\times10^5$ cm^{-1} consistent with the WH analysis. The TD density was 4–5 $\times10^{10}$ cm^{-2} for g=11$\bar{2}$0 and 3–4$\times10^{10}$ cm^{-2} for g=0002 (describing dislocations only with c-component) as measured by plan-view TEM. The TD density was also determined from the film grown at T=405 °C, which had identical SF density but quite different crystal mosaic tilt. With a lower TD density of 3–4$\times10^{10}$ cm^{-2} for g=11$\bar{2}$0 and 2–3 $\times10^{10}$ cm^{-2} for g=0002 and smaller crystal mosaic tilt in this sample, this indicates a possible correlation between TD density and crystal mosaic tilt, in consistence with c-plane group-III nitrides.[26]

The authors acknowledge the fruitful discussions with Professor C. Van de Walle (UCSB) and the support of AFOSR (D. J. Silversmith, program manager) and SSLEC (UCSB). The experimental work made use of the MRSEC facilities at UCSB (supported by the NSF).

[1]J. Wu, W. Walukiewicz, K. M. Yu, J. W. Ager, E. E. Haller, H. Lu, W. J. Schaff, Y. Saito, and Y. Nanishi, Appl. Phys. Lett. **80**, 3967 (2002).
[2]S. P. Fu and Y. F. Chen, Appl. Phys. Lett. **85**, 1523 (2004).
[3]T. B. Fehlberg, G. A. Umana-Membreno, B. D. Nener, G. Parish, C. S. Gallinat, G. Koblmüller, S. Rajan, S. Bernardis, and J. S. Speck, Jpn. J. Appl. Phys., Part 2 **45**, L1090 (2006).
[4]J. Wu and W. Walukiewicz, Superlattices Microstruct. **34**, 63 (2003).
[5]T. Takeuchi, C. Wetzel, S. Yamaguchi, H. Sakai, H. Amano, I. Akasaki, Y. Kaneko, S. Nakagawa, Y. Yamaoka, and N. Yamada, Appl. Phys. Lett. **73**, 1691 (1998).
[6]C. G. Van de Walle and D. Segev, J. Appl. Phys. **101**, 081704 (2007).
[7]H. Lu, W. J. Schaff, L. F. Eastman, J. Wu, W. Walukiewicz, V. Cimalla, and O. Ambacher, Appl. Phys. Lett. **82**, 1736 (2003).
[8]I. Mahboob, T. D. Veal, C. F. McConville, H. Lu, and W. J. Schaff, Phys. Rev. Lett. **92**, 036804 (2004).
[9]P. A. Anderson, C. H. Swartz, D. Carder, R. J. Reeves, S. M. Durbin, S. Chandril, and T. H. Myers, Appl. Phys. Lett. **89**, 184104 (2006).
[10]A. Chakraborty, B. A. Haskell, S. Keller, J. S. Speck, S. P. DenBaars, S. Nakamura, and U. K. Mishra, Appl. Phys. Lett. **85**, 5143 (2004).
[11]M. C. Schmidt, K. C. Kim, H. Sato, N. Fellows, H. Masui, S. Nakamura, S. P. DenBaars, and J. S. Speck, Jpn. J. Appl. Phys., Part 2 **46**, L126 (2007).
[12]K. Okamoto, T. Tanaka, M. Kubota, and H. Ohta, Jpn. J. Appl. Phys., Part 2 **46**, L820 (2007).
[13]D. Segev and C. G. Van de Walle, Europhys. Lett. **76**, 305 (2006).
[14]H. Lu, W. J. Schaff, L. F. Eastman, J. Wu, W. Walukewiecz, V. Cimalla, and O. Ambacher, Appl. Phys. Lett. **83**, 1136 (2003).
[15]Y. Kumagai, A. Tsuyuguchi, H. Naoi, N. Ha, and Y. Nanishi, Phys. Status Solidi B **243**, 1468 (2006).
[16]Y. G. Cao, M. H. Xie, Y. Liu, S. H. Xu, Y. F. Ng, H. S. Wu, and S. Y. Tsong, Phys. Rev. B **68**, 161304 (2003).
[17]G. Koblmüller, C. S. Gallinat, and J. S. Speck, J. Appl. Phys. **101**, 083516 (2007).
[18]C. S. Gallinat, G. Koblmüller, J. S. Brown, S. Bernardis, J. S. Speck, G. D. Chern, E. D. Readinger, H. G. Shen, and M. Wraback, Appl. Phys. Lett. **89**, 032109 (2006).
[19]K. Xu and A. Yoshikawa, Appl. Phys. Lett. **83**, 251 (2003).
[20]Y. J. Sun, O. Brandt, and K. H. Ploog, J. Vac. Sci. Technol. B **21**, 1350 (2003).
[21]M. McLaurin, T. E. Mates, F. Wu, and J. S. Speck, J. Appl. Phys. **100**, 063707 (2006).
[22]A. Hirai, B. A. Haskell, M. B. McLaurin, F. Wu, M. C. Schmidt, K. C. Kim, T. B. Baker, S. P. DenBaars, S. Nakamura, and J. S. Speck, Appl. Phys. Lett. **90**, 121119 (2007).
[23]T. V. Shubina, S. V. Ivanov, V. N. Jmerik, D. D. Solnyshkov, V. A. Vekshin, P. S. Kop'ev, A. Vasson, J. Leymarie, A. Kavokin, H. Amano, K. Shimono, A. Kasic, and B. Monemar, Phys. Rev. Lett. **92**, 117407 (2004).
[24]M. B. McLaurin, A. Hirai, E. Young, F. Wu, and J. S. Speck, Jpn. J. Appl. Phys. **47**, 5429 (2008).
[25]X. Wang, S.-B. Che, Y. Ishitani, and A. Yoshikawa, J. Appl. Phys. **99**, 073512 (2006).
[26]V. Srikant, J. S. Speck, and D. R. Clarke, J. Appl. Phys. **82**, 4286 (1997).